27
4-30-79

UCRL-52607

NUMERICAL SIMULATION OF TORNADO-BORNE MISSILE IMPACT ON REINFORCED CONCRETE TARGETS

D. K. Tu
R. Larder

February 1979

This work was supported by the U.S. Nuclear Regulatory Commission under Interagency Agreement DOE 40-550-75 with the U.S. Department of Energy.

LAWRENCE LIVERMORE LABORATORY
University of California Livermore, California 94550

UCRL-52607

NUMERICAL SIMULATION OF TORNADO-BORNE MISSILE IMPACT ON REINFORCED CONCRETE TARGETS

D. K. Fu
CAI Engineering, Berkeley, CA
R. Larder
Lawrence Livermore Laboratory, Livermore, CA

MS. date February 1979

CONTENTS

LIST OF ILLUSTRATIONS

LIST OF TABLES

ABSTRACT

This study is a continuation of the Lawrence Livermore Laboratory (LLL) effort to evaluate the applicability of using the finite element procedure to numerically simulate the impact of tornado-borne missiles on reinforced concrete targets.

The objective of this study is to assess the back-face scab threshold of a reinforced concrete target impacted by deformable and nondeformable missiles. Several simulations were run using slug and pipe-type impacting missiles. The numerical results were compared with full-scale experimental field tests.

ACKNOWLEDGMENTS

We wish to thank Dr. Lynn Seaman, Stanford Research Institute (SRI), for his discussion on work he is doing for Electric Power Research Institute, which is similar in scope to ours.

Particularly, we wish to thank Dr. Jim Costello, U.S. Nuclear Regulatory Commission, Office of Standards Development, for his guidance, discussions, and support throughout this study.

INTRODUCTION

In recent years, the nuclear industry and its regulatory agency have intensified their efforts in reexamining their analytical procedures[1,2] for the design of structural barriers for tornado-borne missiles. A number of full-scale experimental test programs[3-7] (i.e., impacting typical nuclear power plant wall and roof slabs with selected design tornado-borne missiles) have been completed. These full-scale test programs have brought forth new perceptions to the impact problem. The test programs have also established important data points from which the validity of existing empirical analytical procedures can be assessed.

To extend the data further with more full-scale tests is impractical because of cost considerations. With the uncertainties of extrapolating the available test data beyond the test parameters, it is desirable to supplement the full-scale tests with analytical methods. The tasks now are to develop an analytical method that will incorporate the appropriate properties and considerations, and to match existing large-scale test results and make reasonable extensions beyond the test conditions.

This study is a continuation of the efforts by Lawrence Livermore Laboratory (LLL) to evaluate the applicability of using the finite element method to numerically simulate the impact of tornado-borne missiles on reinforced concrete targets. In the first report, Numerical Simulation of Tornado-Borne Missile Impact[8] reasonable comparisons were made between the finite element method and experimental results of the reinforced concrete target's back-face scab damage. The study focused on the numerical simulation of solid slug (rigid) missile impacts. The calculations were compared with two of the Calspan Corporation's large-scale experimental tests.[4]

In reviewing the literature[9,10] as part of the first study, two computational models describing the dynamic behavior of concrete were found and used to model the concrete target. Based on several trial calculations,

it was found that the steel reinforcements responding in tension could be appropriately modeled by altering the equation of state for the concrete, i.e., the steel bars are smeared in the concrete zones and the key values defining the equation of state in tension are dependent on the strength and the percentage of the steel reinforcements.

The first study concluded that the finite element method is an appropriate analytical tool to evaluate the back-face scab damage profile of reinforced concrete targets impacted by rigid type missiles.

OBJECTIVES

The large-scale experimental test results[3] have shown that local response of the target structure is the dominant mode of behavior. The key to the design of a structural barrier against local effects of a tornado-borne missile is to be able to identify if scabbing of the back face of the target will or will not occur. Although there is a degree of scabbing that could be allowed without damage to internal systems, e.g., equipment, piping system, etc., it is conservative to establish a criteria of no scabbing. Currently no analytical method exists that can accurately portray completely the total load response (Fig. 1).

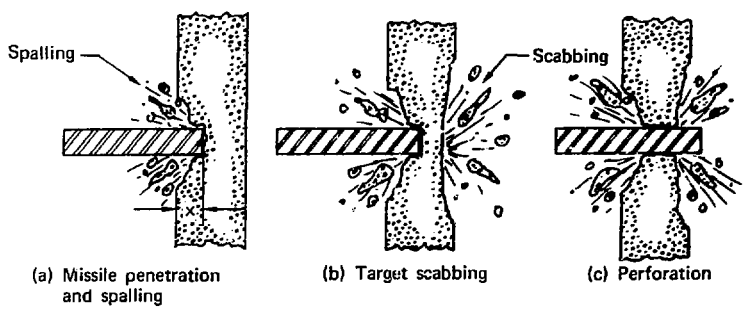

FIG. 1. Sequence of the load response.

Our first study[8] showed that the finite element method can be used to assess the back-face scab threshold of a reinforced concrete target impacted by a rigid missile. The objectives of this effort are to make further refinements in the concrete constitutive model and finite element geometry, to study the sensitivity of the back-face scab to steel reinforcement and impacting missile velocity, and to extend the finite element method to deformable type missiles.

ANALYTICAL PROCEDURE

The finite element program selected to perform the numerical calculations is entitled DYNA2D.[11] DYNA2D is designed to calculate large deformation, elastic and inelastic dynamic transient response of plane or axisymmetric bodies. DYNA2D capabilities that are relevant to this project include:

- Shock-interface conditions to set correctly the velocity along the contact surface after a void closes.
- Sliding-material interfaces that allow sliding, but not penetration.
- Tied-material interfaces that allow unequal zoning across the interface, but not sliding.
- Higher order elements.

In general, DYNA2D uses either the finite element method or finite difference method to generate the spatial grid. The finite element option was used for this study. Because of the interest in short duration loads and effects in the earliest part of the transient response, an explicit time integration scheme is used. Artificial viscosity is employed along with the explicit scheme to control the development of shocks that occur in impact problems. The equations of motion are integrated using the central difference method.

MATERIAL MODELS

To be able to solve the equations of motion, it is necessary to define the constitutive models that describe the behavior of the impacting materials, i.e., the reinforced concrete for the target and the steel for the missile. Selected to describe the impacting missile is a von Mises constitutive model available in the DYNA2D program. The von Mises model with a simple isotropic hardening law has been widely and successfully used.

The concrete model is an adaptation of the generalized plasticity model for predicting the failure of concrete which was developed by Gupta and Seaman[12] of SRI International, under contract with Electric Power Research Institute. The steel reinforcements in the concrete are represented by an increase in the tensile-yield value of the associated concrete layer.

MISSILE

An elastic-plastic, stress-strain relationship[13] is employed to represent the missile material composition. For the stress states interior to the yield surface, the behavior is elastic and isotropic. Yielding of the material is determined by a von Mises criterion with a hardening behavior that is a linear combination of isotropic and kinematic.

Figure 2 shows the typical behavior of the ductile metal missile loaded first in uniaxial tension and followed by uniaxial compression. Straight line approximations characterize the elastic modulus, E, and the strain hardening modulus, E_t. The hardening parameter, β, is used to describe the hardening behavior where (a) kinematic hardening is obtained with $\beta = 0$, (b) isotropic hardening is obtained with $\beta = 1$, and (c) a linear combination of the two is obtained for β between zero and 1.

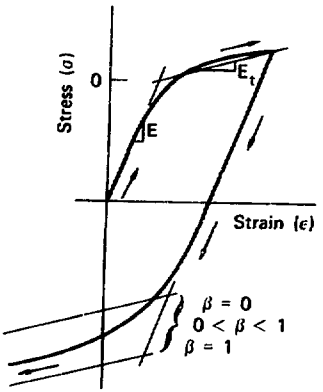

FIG. 2. Typical stress-strain behavior of a ductile metal bar.

TARGET

The material model for concrete encompasses two major physical behaviors: (a) irreversible compaction of voids, and (b) shear strength, which is sensitive to confining pressure. The DYNA2D material subroutine, entitled soil and crushable foam, models these characteristics using an elementary isotropic plasticity theory.

Concrete exhibits a behavior that is pressure dependent. Because of the high porosity of concrete, the material crushes under pressure with an irreversible path. Furthermore, the pressure affects the shear yielding which, in turn, affects the compaction. To handle the shear and compaction behavior, two yield surfaces are used to describe the general behavior of concrete. The two yield surfaces in stress space are shown in Fig. 3. The shear yield surface, which allows for the increase in shear strength with confining pressure, is a surface of revolution centered about the hydrostat with the open end pointing

toward the compression. The second surface, which describes the compaction and the influence of shear stress, caps the shear yield surface at right angles to the hydrostat. The deviatoric part is elastic-perfectly plastic so the surface of revolution is stationary. The volumetric part has variable strain hardening so the end plane moves outward during volumetric yielding.

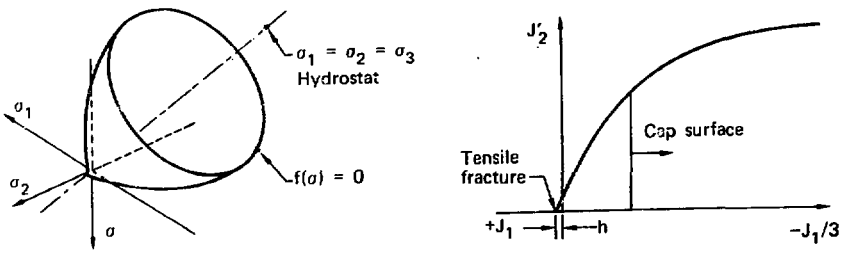

(a) Shear yield surface in stress space

(b) Cap surface in stress space
J_1 = first invariant of the stress tensor
J'_2 = second invariant of the deviatoric stress tensor

FIG. 3. Yield surface in stress space.

Within the region bounded by the two surfaces, the concrete behaves elastically. When the yield surface is reached, plastic deformation occurs. Tensile behavior is postulated as an extension of the curvature of the shear yield surface. The intersection of the shear yield surface with the hydrostat is where tensile fracture of the concrete occurs. Numerically, once the main stress reaches the tensile cutoff (fracture) value, it is assumed to remain there until unloading occurs.

Shear Yield Surface

The shear yield surface is defined by a yield function of the form

$$f_1 = \sqrt{J_2'} - \left[A_1 + A_2 \exp\,(J_1/A_3) + A_4 \exp\,(J_1/A_5)\right] = 0 \quad , \tag{1}$$

where

J_1 = first invariant of the stress tensor

J_2' = second invariant of the deviatoric stress tensor

A_1-A_5 = coefficients determined experimentally.

The form of the shear function is selected from the computational and experimental work of Gupta and Seaman at SRI. The DYNA2D soil and crushable foam model initially permitted a shear yield surface defined by a polynomial function of pressure. This polynomial function was replaced by the SRI exponential function and offers several advantages. One advantage is that it makes it much easier to vary the tension cutoff. Another advantage is the correlation with experimental data already established by SRI.

Cap Surface

The volumetric hardening is described by

$$f_2 = P - f(\varepsilon_{KK}) \quad .$$

For loading, $f_2 \geq 0$, and the volume strain rate; $\dot{\varepsilon}_{KK} \leq 0$, increasing compression

$$P = f(\varepsilon_{KK}) \quad .$$

The function, f, which describes the pressure-volume strain behavior, is shown in Fig. 4.

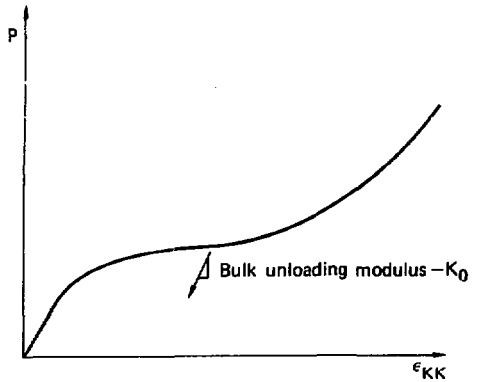

FIG. 4. Typical pressure-volume strain behavior.

The shear yield function (f_1) and the cap surface function (f_2) are shown in Fig. 5. The solid lines represent shear and compaction yield for concrete and contrast the von Mises yield surface shown by the dotted line.

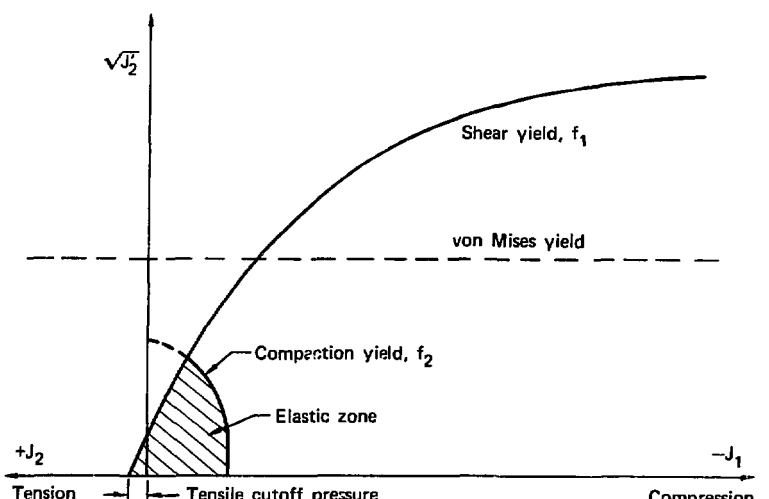

FIG. 5. Typical yield surfaces in $\sqrt{J_2'} - J_1$ space.[14]

FAILURE CRITERIA

The impact of an oncoming missile induces compressive shock waves on the front face of the target structure. The shock waves propagate through the thickness and reflect off the rear free surface as tensile waves. At the rear free surface, if the algebraic sum of the oncoming compression waves and the reflected tension waves exceeds the tensile capacity of the concrete, scabbing of the concrete is expected.

Limited information is available about the behavior of concrete in multistress states, especially in tension. To be able to assess back-face scab damage, three tensile criteria are tested against the calculations and experimental data: (a) mean stress cutoff, (b) effective strain, and (c) strain energy.

With the first criterion, tensile failure is assumed to occur when the mean stress value reaches the root value of the shear yield function, i.e., the value of J that satisfies Eq. 1, when $J_2 = 0$. This tensile cutoff is shown in Fig. 5. The effective strain criterion requires that the mean stress is tensile, and the maximum tensile stress and the accumulated effective strain exceed threshold values before tensile failure is assumed.

The third criterion is based on work by Birkimer and Lindeman[15] using the strain energy in the stress wave to establish tensile failure. Birkimer shows with uniaxial tests that the total energy at tensile fracture is independent of the strain rate. The strain energy is calculated to be

$$U = \frac{AEC}{2} \int_{t_1}^{t_2} \varepsilon^2 dt \quad ,$$

where

U = strain energy
A = cross-sectional area

E = Young's modulus of elasticity

C = seismic velocity

ϵ = strain.

Relating the strain energy to tensile yield,

$$U = \frac{AC}{2E} \int_{t_1}^{t_2} \sigma^2 dt \quad .$$

Ignoring the elastic energy and equating the strain energy to time, tensile fracture can be determined based on the duration of the mean stress at the threshold value. The total duration of threshold value for scabbing to occur is given by

$$T_{scab} = \frac{2U'E}{\sigma_y^2 C} \quad ,$$

where

T_{scab} = total time duration for scabbing to occur

U' = strain energy per unit area

σ = stress.

The quality of the three criteria, as they were applied to determining scab damage, was unknown at the outset of the study. Therefore, each calculation was tested against the three criteria. Selected calculations that corresponded to experimental field tests were benchmarked to the test observations using the three criteria.

STUDY PROBLEMS

The objectives of this study have been pursued by analyzing three different groups of problems. In the first group (Group A), sensitivity of the back-face damage was evaluated for steel reinforcement strengths and for missile velocities. The impacting missile was classified as nondeformable. In the next two groups (Groups B and C), the effects of a deformable missile were evaluated. These two groups used the same target configuration and material properties as the first group, but they used different length and diameter pipe missiles.

MATERIALS PROPERTIES

The properties of the missile were assumed as follow:

$E_0 = 3.0 \times 10^7$ psi $\qquad \sigma_{yield} = 40{,}000$ psi

$E_t = 1.0 \times 10^7$ psi $\qquad \nu = 0.27.$

The material is taken to harden isotropically.

The pressure-volumetric strain curve used to describe the cap surface of the concrete model is shown in Fig. 6. The curve was extracted from SRI work[14] for stress-strain behavior for hydrostatic loading. Unloading was assumed to occur along the elastic bulk modulus, K_0.

The coefficients A_1 - A_5, describing the shear yield surface, are tabulated in Table 1. SRI calculated the two sets of coefficients:[12] (a) one set was obtained by fitting the static triaxial data on concrete, and (b) the other was established from one-dimensional plate impact experiments. The dynamic model was taken to have the same shape as the static model. In general, the concrete is stronger and stiffer under dynamic loading conditions.

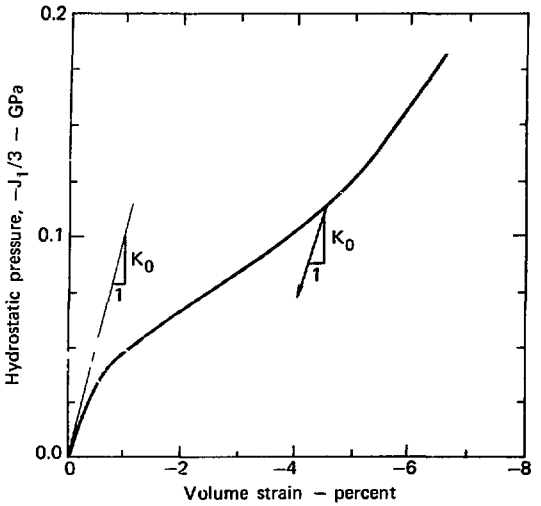

FIG. 6. Pressure-volume strain behavior for hydrostatic loading.

TABLE 1. Shear yield function parameters.

Parameters	Static (psi)	Dynamic (psi)
A_1	13053.0	15084.0
A_2	-12038.0	-12038.0
A_3	39160.0	39160.0
A_4	- 256.7	- 411.9
A_5	1015.3	2900.8

The properties of the target were assumed as follows:

$K_0 = 3.25 \times 10^6$ psi $\qquad G_0 = 2.34 \times 10^6$ psi

$\nu = 0.21 \qquad \gamma_m = 2.25 \times 10^{-4} \frac{\text{lb-s}^2}{\text{in.}^4}$.

GEOMETRY

The geometry and layout of the elements for the three problem groups are shown in Fig. 7. The target is a circular plate 132 in. in diameter and 12 in. thick. The impact time duration is short in comparison to the fundamental frequency of the target structure; therefore, the response of the target structure is isolated to the area of the impact zone. In all three groups, the simple support boundary condition is assumed.

The target structure is divided into 12 rows through the thickness. Each row is further divided into columns, each having a smaller length at the impact area and gradually increasing toward the boundaries, as shown in Fig. 8.

For the two problem groups using pipe as the impacting missile, a more refined mesh is zoned for the impact area of the target structure. The finer mesh is necessary because the impacting pipe missile wall thickness is relatively small in comparison to the length of the general grids describing the target structure. A tied-material interface option is used to allow for the unequal zoning.

Three types of impacting missiles are used: (a) an 8-in.-diameter steel slug with a 12-in. length; (b) an 8-in.-diameter pipe with a 7-ft length and 0.44-in. wall thickness; and (c) a 12-in.-diameter pipe with a 13.5-ft length and 0.40-in. wall thickness.

As the deformation of the steel slug is anticipated to be small and of secondary interest, a coarser grid is used to model the missile. To provide proper distribution of the velocity at impact, higher order elements are used to describe the nose of the slug missile.

For the pipe missiles, three equidistant columns divide the thickness. Each column is divided into rows, with the aspect ratio in the frontal region equal to 1 and the aspect ratio gradually increasing toward the rear of the missile.

All the impacting missiles are initially separated from the target structure by a 0.002-in. gap.

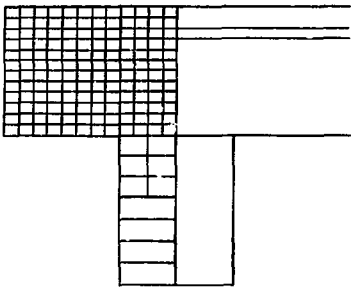

(a) 8—in. o d. steel slug missile

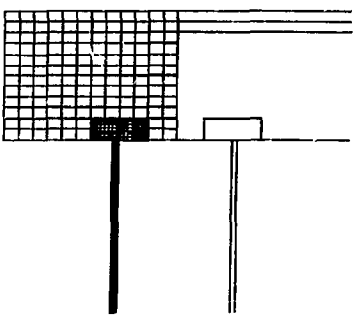

(b) 8—in. o.d. steel pipe

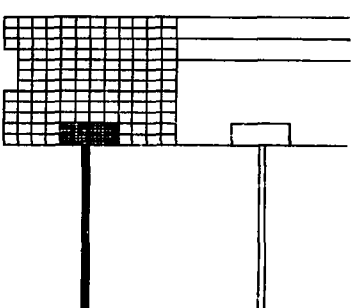

(c) 12—in. o.d. steel pipe

FIG. 7. Geometry and layout of the finite element models at the impact area.

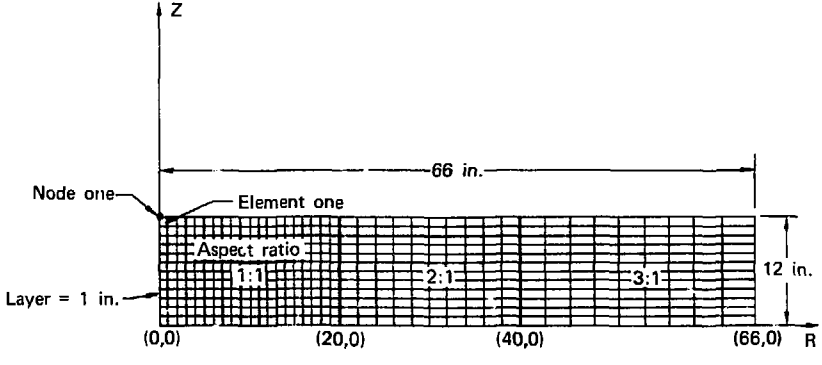

FIG. 8. Lagrange target structure grid (8-in. Ø stem slug calculation).

RESULTS

Three groups of numerical simulations were conducted to study the sensitivity of back-face scab damage:

- Group A studied the sensitivity of damage to steel reinforcement and the damage due to the impacting velocities of a slug missile.
- Group B studied the damage due to the impacting missile velocities of an 8-in.-diameter pipe.
- Group C studied the damage due to the impacting missile velocities of a 12-in.-diameter pipe.

To make these numerical simulations within reasonable computer costs, it was concluded after examining the calculated time histories that scab damage could be assessed by examining the first 0.5 ms of the target structural response after impact. The mean stress and effective strain criteria can be readily assessed within the 0.5-ms time frame. With the strain energy criterion, which is dependent on the accumulated duration of the mean stress at the tension cutoff value, the selection of the total time frame is important.

Based on the numerical simulation of the slug missile impact in the previous study, the 0.5-ms time frame is judged to be a reasonable limit. Within the 0.5-ms time frame, the range of computed velocities of the back-face nodes are comparable to the maximum measured scab velocities in the full-scale tests. Beyond the selected time frame, predicted scab velocities decreased significantly and would not compare with the observations made on the full-scale tests.

GROUP A

Steel Reinforcement

The impacting missile was an 8-in.-diameter steel slug weighing 200 lb. The dynamic model for the concrete shear yield surface was used (see Table 1). The tension cutoff value was 1378 psi.

To study the sensitivity of the back-face scab damage as a function of the steel reinforcement, the missile parameters were set constant and one general concrete model was used. Only the tension cutoff value of the representative layer of the steel reinforcement was varied.

Three tension cutoff values for the representative rebar layer were studied. Tension cutoff values are established by varying the coefficients A_4 and A_5 of the shear yield function so that the function will cross the hydrostat at the desired values, as shown in Fig. 9. The selected cutoff values are listed in Table 2. The first study case (case SR13) represents no steel reinforcement in the target structure. The second and third cases represent progressively higher percentages of steel reinforcement. The missile velocity was set to impact on 122 fps, corresponding to the full-scale test.

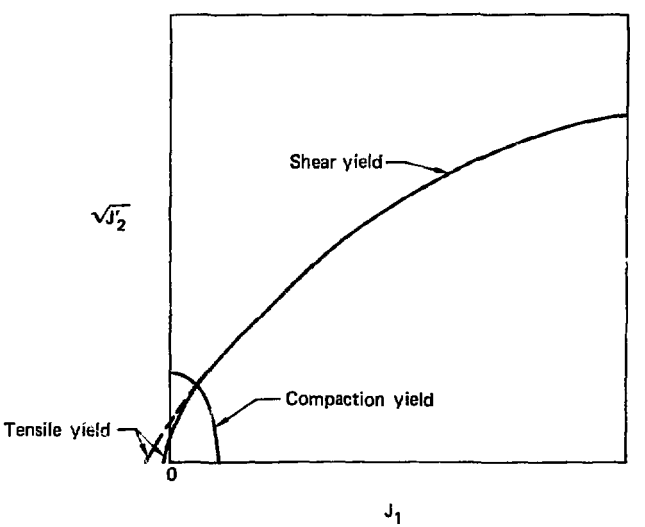

FIG. 9. Shear yield function (tension cutoff variation).

TABLE 2. Group A tension cutoff values.

Case	Tension cutoff values (psi)
SR13	1378
SR20	2000
SR25	2500

A full-scale test experiment (Test No. 4F) using a steel slug as the impacting missile was conducted by Calspan.[4] The finite element model for the impacting missile in Group A is similar in dimension to the test missile in Test No. 4F. The actual missile weighed 214 lb. The target structure is 12-in. thick. It is assumed that the effect of unconfined compressive concrete strength, f'_c, is insignificant. This assumption is supported by experimental tests conducted by Sandia Laboratories[3] in its study of the effect of concrete strength on impact response.

The results of Calspan Test No. 4F show the impacting missile velocity of 122 fps to be greater than the scab threshold. The scab damage penetrated slightly below the back-steel reinforcement layer. The maximum measured scab velocity was 25 fps.

Using the mean stress or effective strain time histories of the back-face elements, the time of failure can be determined using any of the three criteria. Once the time of failure is determined, the maximum scab velocity can be found by correlating the time to the respective nodal velocity time histories. Maximum scab velocities are shown in Table 3 for each of the following criteria.

TABLE 3. The effect of rebar tension cutoff on potential scab velocities.

Case	Mean stress (fps)	Effective strain (fps)	Strain energy (fps)
SR13	22.9	7.5	30.4
SR20	16.3	8.3	30.0
SR25	19.2	9.2	27.5

Mean Stress Criteria. Findings based on the mean stress criteria show minimal differences between the three cases. The maximum scab velocity for the three cases range from 16 to 23 fps. Fracture of the back-face elements in direct line with the missile occurs within the first 0.1 ms. The back-face area with the potential for scabbing at the highest velocity is a circumferential area located 1 diameter from the centerline of impact.

Effective Strain Criteria. The back-face scab velocity increases with the increasing tension cutoff value of the representative rebar layer. The earliest time when fracture is predicted to occur is approximately 0.12 ms for all three cases. The scab velocity for case SR20 is about 12% greater than for case SR13. For case SR25, it is about 21% greater than that predicted for case SR13.

The back-face area with the greatest potential scab velocity is an area 0.5 to 1 diameter from the centerline of impact. The maximum scab velocity predicted for SR25 is 12.5 fps.

Strain Energy Criteria. With the strain energy criteria, the back-face elements directly in front of the impact have the greatest potential for scabbing. As the tension cutoff value of the representative rebar layer is increased, the time of scabbing is delayed. The predicted maximum scab velocity for all three cases varied only slightly. The maximum scab velocity ranges from 27 to 30 fps. The potential for scabbing rapidly decreases as the distance from the centerline of impact increases.

The mean stress criteria and the strain energy criteria indicate that the potential for scabbing is not sensitive to the steel reinforcement in the rear face of the target structure. With the mean stress criteria, scabbing occurs early in the target response. The strain energy criteria predicts scabbing to occur approximately 0.4 ms after impact. As compared to the experimental result, the mean stress criteria tend to predict a slightly lower maximum scab velocity, and the strain energy criteria predict it slightly higher. The nonmonotonic variation in scab velocity with concrete strength for the mean stress criteria reflects the variability of the results with these criteria.

The effective strain criteria do not compare well with the experimental results. The predicted maximum scab velocity is less than the experimental measured maximum scab velocity of 25 fps.

Both the mean stress criteria and the effective strain criteria predicted the maximum scab velocity to occur in back-face elements away from the centerline of impact. The strain energy criteria predicted the maximum scab velocity to occur in the back-face elements directly in front of the impacting missile. The conical shape damage profile of Test No. 4F indicates that the maximum scab velocity would occur in the scabbing material directly in front of the impacting missile. Based on these comparisons, the strain energy failure criteria appear to be the best.

Missile Velocities

The impacting missile was an 8-in.-diameter steel slug, weighing 200 lb. The dynamic model for the concrete yield surface was used (see Table 1). The tension cutoff for the concrete was 1378 psi. The representative rebar layer tension cutoff was 2000 psi.

Four numerical simulations were conducted to study the sensitivity of the back-face scab damage to impacting missile velocity. The corresponding impacting missile velocities for the four numerical simulations are shown in Table 4. In the first case, MV4F, the impacting missile velocity of 122 fps

is the same as the missile velocity for Calspan Test No. 4F. As noted earlier, the missile velocity of 122 fps is greater than the scab threshold for a 12-in.-thick target structure.

TABLE 4. Group A missile velocities.

Case	Velocity (fps)
MV4F	122.0 (0%)
MV10	109.8 (-10%)
MV20	97.6 (-20%)
MV40	73.2 (-40%)

In the other three simulations, the missile velocities selected are incremental decreases to the missile velocity of case MV4F. For example, the missile velocity for case MV40 is 73.2 fps, which is 40% less than the case MV4F missile velocity.

The maximum scab velocities for these calculations are shown in Table 5 for each of the following criteria.

TABLE 5. The effect of missile impact velocity on potential scab velocities.

Case	Mean stress (fps)	Effective strain (fps)	Strain energy (fps)
MV4F	16.3	9.1	30.0
MV10	15.8	12.0	23.3
MV20	20.4	11.0	19.2
MV40	15.0	9.2	14.1

Mean Stress Criteria. The maximum scab velocities predicted by the mean stress criteria varied insignificantly in all four cases. For case MV4F, the predicted maximum scab velocity is 16 fps, which is slightly greater than predicted maximum scab velocity of 15 fps for case MV40. The predicted response based on the mean stress criteria is not sensitive to any variation of the impacting missile velocity.

Effective Strain Criteria. No consistent trend of predicted maximum scab velocity based on the effective strain criteria was found for the four cases. In general, the predicted maximum scab velocities were less than expected.

Strain Energy Criteria. Predictions based on the strain energy criteria show a definite trend corresponding to the impacting missile velocity. For case MV4F, the maximum calculated scab velocity is 30.0 fps. As the impacting velocity decreases, the maximum scab velocity and the potential back-face scab damage area decrease.

Figures 10 and 11 show the pressure-time histories and axial stress-time histories, respectively, of element 422, which is located at the front impact region of the target. These figures, which represent cases MV4F and MV40, show the decrease in the maximum pressure and axial stresses with decreasing missile impact velocity. They also show the decrease in time duration of the interface stresses with decreasing missile impact velocity.

In comparison to case MV4F, case MV10 with a 10% decrease in impacting velocity has a predicted maximum scab velocity that is 22% less. For case MV20 whose impacting velocity is 20% less than case MV4F, the predicted maximum scab velocity is 36% less. For case MV40, the impacting velocity is 40% less, and the predicted maximum scab velocity is 52% less in comparison to case MV4F. The damage area for case MV40 is limited to one back-face element, which would indicate the scab threshold limit was reached.

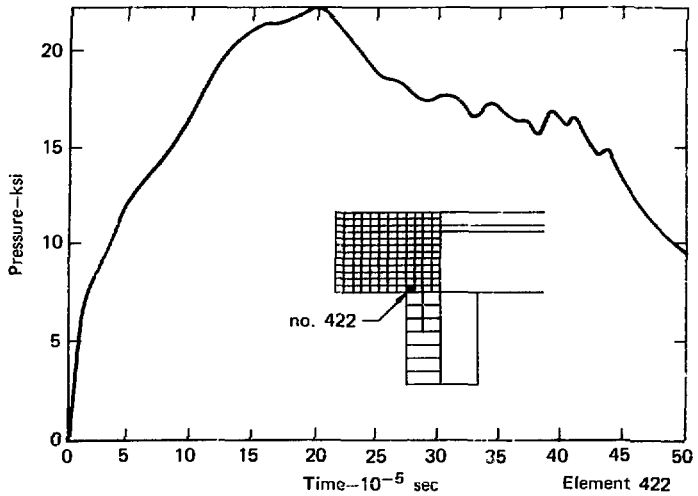

(a) Case MV4F: Impact velocity–122 fps

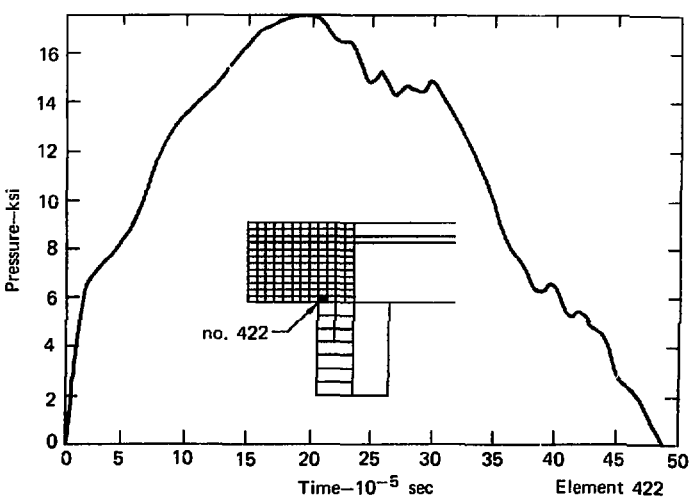

(b) Case MV40: Impact velocity–73.2 fps

FIG. 10. Pressure-time histories (front impact region).

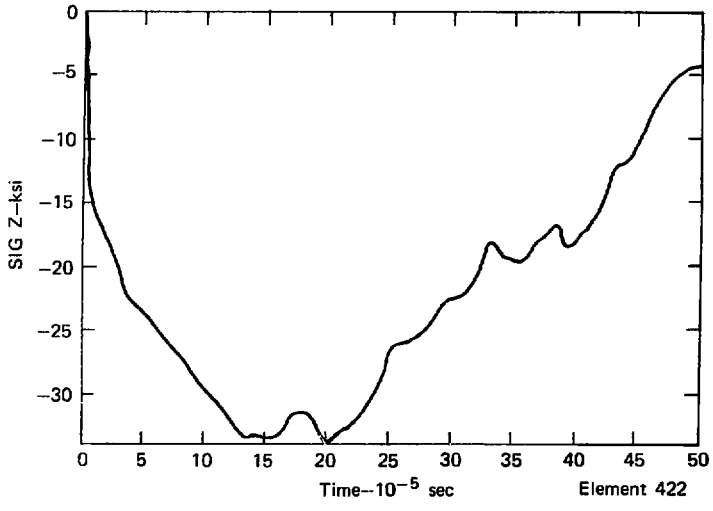

(a) Case MV4F: Impact velocity–122 fps

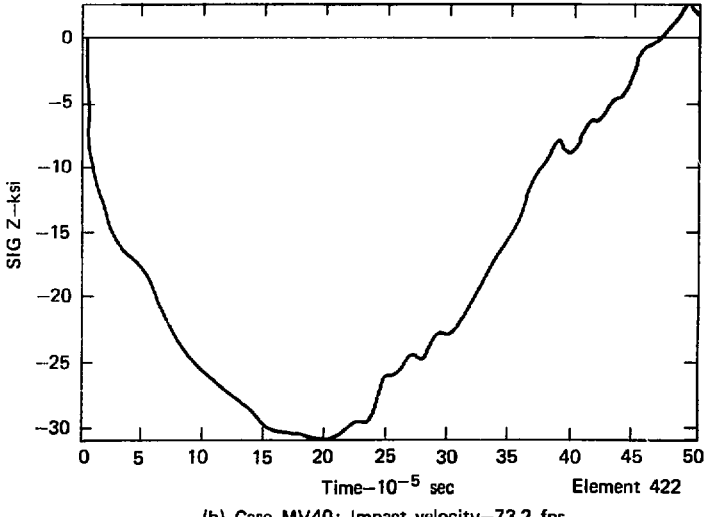

(b) Case MV40: Impact velocity–73.2 fps

FIG. 11. Axial stress-time histories (front impact region).

GROUP B

The impacting missile was an 8-in.-diameter pipe weighing 200 lb. The dynamic model for the concrete shear yield surface was used (see Table 1). The tension cutoff value was 1378 psi. The representative rebar layer had a tension cutoff of 2000 psi.

In the Calspan full-scale test program, two tests were conducted using 8-in.-diameter pipe as the impacting missile. The pipe missile weighed 202 lb and was 7-ft long. The tests, Test No. 15F and Test No. 16F, had impacting velocities of 135 fps and 209 fps, respectively. The target structure was a 12-in.-thick reinforced concrete wall.

For Test No. 15F, the impacting velocity was less than the scab threshold. The missile sustained negligible deformation. Front-face damage to the target structure was observed. Radial cracks were observed in the back-face.

For Test No. 16F, the impacting velocity was greater than the scab threshold. Minor front-face deformation occurred. Considerable front-face damage of the target structure was observed. The back-face had extensive scab damage with a maximum measured scab velocity of 40 fps. It should be noted that in the experimental program, Test No. 16F was conducted following Test No. 15F on the same target plate. It is not known what effect the damage from the initial impact had on the subsequent impact.

Two series of numerical calculations were conducted using the 8-in. pipe as the impacting missile. The first series studied the effect of the rebar layer on the target structural response for a pipe missile impact. Similar to the slug missile study (Group A), the conclusion of the first of the numerical simulations is that the rebar layer has limited influence on the target response in the first 0.5 ms after impact.

The second series of numerical simulations studied the potential for back-face scab damage as a function of the oncoming missile velocity. Six case studies were conducted. The corresponding impact velocities for each case are listed in Table 6. The full-scale test, Test No. 15F, correlates to Case 8D15F, and

both have the same impacting missile velocities. The Test No. 16F missile velocity ranges between the Case 8D50 and Case 8D60 velocities, which are 202.5 fps and 216.0 fps, respectively.

TABLE 6. Group B missile velocities.

Case	Velocity (fps)
8D15F	135.0
8D10	148.5
8D30	175.5
8D50	202.5
8D60	216.0
8D80	243.0

Evaluating the nodal and element time histories of the back-face elements in the six case studies, small changes in the stress states, nodal velocities, and nodal accelerations were observed despite the increase of the impacting velocity of the missile. Figure 12 shows the pressure-time histories of element 411, which is at the back face of the target in line with the centerline of impact. As can be seen, there are no significant changes in the time histories despite the large difference in the impact velocities of the two cases. The tension cutoff value was not reached in any of the six cases, although in two of the cases, Case 8D60 and Case 8D80, the missile velocities were greater than the impacting velocity of Test No. 16F, which had extensive back-face damage. The mean stress criteria and the strain energy criteria could not be applied because the tension cut-off stress was not reached.

The effective strain criteria predicted scab damage to occur for missile velocities greater than or equal to 175.5 fps (Case 8D30). The predicted maximum scab velocities for Case 8D30 and the three other cases with greater

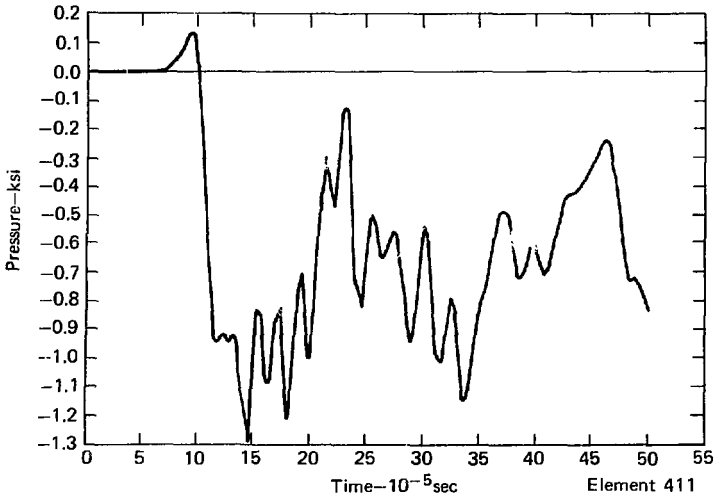

(a) Case 8D15F: Impact velocity–135 fps

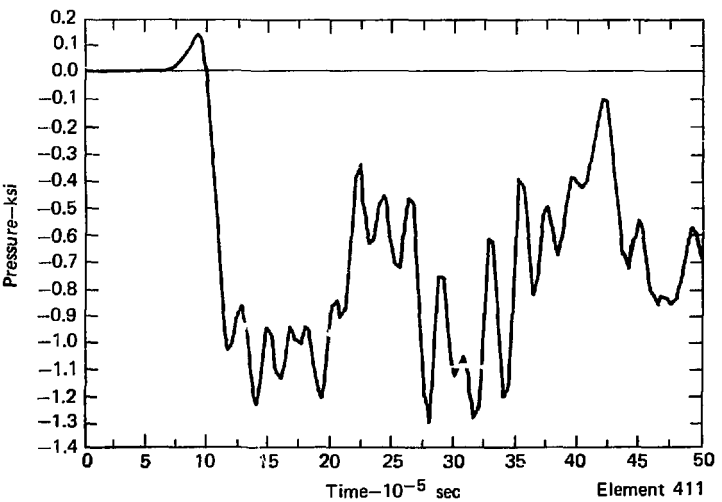

(b) Case 8D80: Impact velociy velocity–243 fps

FIG. 12. Pressure-time histories (back face of target).

impacting velocities ranged from 3.4 to 5.6 fps. The predicted maximum scab velocities corresponded poorly with the measured maximum scab velocity of 40 fps in Test No. 16F.

The inability of the analytical procedure to provide correspondence to the field-test results of an 3-in. pipe missile occurs somewhat because the analytical procedure is unable to account for the initial penetration of the missile. Currently, the procedure produces a premature collapse of the impact face of the missile. The greater stresses resulting from the small contact area of the pipe missile cause considerable front-face spalling, which DYNA2D does not account for. The deformed shape of the missile at 0.48 ms after impact for Case 8D15F is shown in Fig. 13.

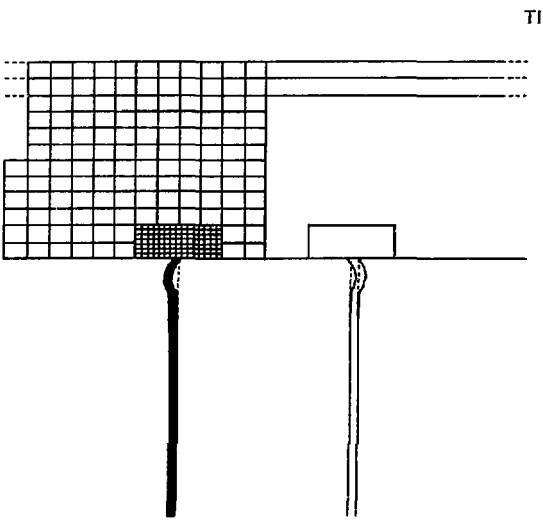

FIG. 13. Deformed shape for missile 0.48 ms after impact (Case 8D15F).

GROUP C

The impacting missile was a 12-in.-diameter pipe weighing 733 lb. The dynamic model for the concrete shear yield surface was used (see Table 1). The tension cutoff was 1378 psi. The representative rebar layer had a tension cutoff of 2000 psi.

Sandia Laboratories conducted a series of full-scale tests using 12-in.-diameter pipe as the impacting missile. The test pipe weighed 743 lb, and was approximately 13.75-ft long. Three of the tests, Test Nos. 10, 11, and 16, were conducted with a 12-in.-thick target wall.

The impacting velocity for Test No. 10 was 143 fps, which was sufficient to perforate the target. Minor damage to the impact face of the missile was observed.

For Test No. 11, the impacting velocity was 98 fps, which proved to be greater than the scab threshold. The missile sustained minor frontal damage. Damage was observed at both the front-face and back-face areas of the target structure. The maximum measured scab velocity was 47 fps.

For Test No. 16, the impacting velocity of 92 fps was at the scab threshold. Considerable front-face damage of the missile was observed. Penetration of the missile into the target structure occurred with some material starting to peel off the back face of the target.

Three case studies were conducted. The corresponding impact velocities for each case are listed in Table 7. The impacting velocities correspond to the Sandia Laboratories test velocities.

TABLE 7. Group C missile velocities.

Case	Velocity (fps)
12D10	143
12D11	98
12D16	92

Similar to the Group B study problems, stress-time histories of the back-face elements varied insignificantly between the three case studies in Group C. The time frame for the numerical calculations was extended to 1 ms in the hope that the longer time period would reveal more information. Unfortunately, the analytical procedure was unable to account for penetration, which in turn caused premature collapse of the missile.

The three failure criteria were applied to the back-face elements of each case. The conclusions were inconsistent with experimental observations. The deformed shape of the missile at 0.98 ms after impact is shown in Fig. 14.

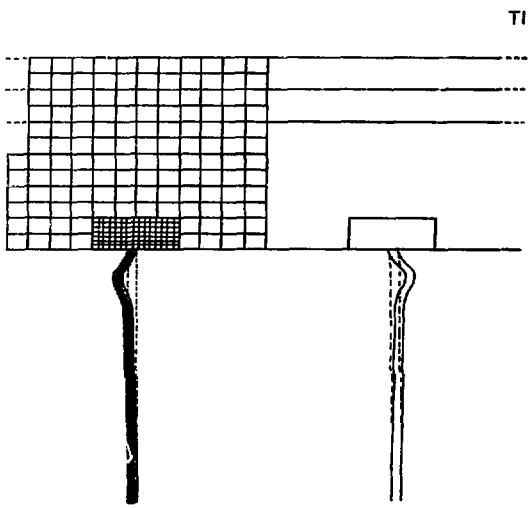

FIG. 14. Deformed shape for missile 0.98 ms after impact (Case 12D10).

CONCLUSIONS

Three groups of numerical simulations were conducted to evaluate the applicability of the finite element method in defining back-face scab damage of the target. Two different types of impacting missiles were considered--deformable and nondeformable. Three failure criteria were formulated to assess back-face scab damage potential. The criteria were benchmarked against experimental observations.

The steel reinforcement study showed that back-face scab potential is insensitive to the addition of steel reinforcement at the rear face. From the deformable missile studies, the numerical procedure appears to be able to predict the deformability effects of impact on the pipe missiles. The buckling of the pipe and postbuckling behavior, as predicted by DYNA2D, appear reasonable.

Because the tensile behavior of concrete under dynamic loading conditions is not well understood, the definition of the behavior was assumed, i.e., the shear yield surface in the tensile region was taken to be an extension of the curvature of the yield surface in compression. The shear yield surface in the compression region was defined by supporting experimental data. The tensile yield cutoff value was selected based on a review of the literature and our best judgment.

Both mean stress criteria and strain energy criteria are dependent on the *tensile cutoff value selected. The assessment of the back-face scab potential* based on these two criteria is sensitive to the selection of the cutoff value. The sensitivity of the tensile value selection was not studied. The effective strain criteria were found to be inappropriate because of the lack of agreement with experimental observation. Until further work is performed to better understand and define the dynamic tensile behavior of concrete, the quality of the numerical results will be suspect.

Based on the previous study and the first group of numerical calculations in this study, the finite element method was judged to provide reasonable correlation to experimental tests for nondeformable-type missile impacts. For deformable-type missile impacts, no comparable correlation was produced. The problem with the finite element procedure used for this study is the inability of the procedure to account for the front-face penetration. The inability to simulate penetration of the missile into the target alters significantly the duration of the interface stress, as well as the length of the stress wave path through the target. The present procedure causes premature collapse of the deformable missile, and does not allow intrusion of the missile into the target. Based on sets of numerical simulations for deformable-type missile impact, it can be seen that the depth of penetration is important in determining the extent of back-face scab damage. Modifications need to be made or added to the finite element procedure to account for impact target face-missile penetration.

Front-face penetration can be handled by incorporating an analog to account for spalling of the front-face elements. The most pressing need lies with the understanding of the principal behavior of concrete under short duration tensile load. Future numerical studies should be complemented with limited material tests to provide the framework for the development of a cost-effective analytical procedure in the evaluation of tornado-borne missile impacts.

CITED REFERENCES

1. Design Basis Tornado for Nuclear Power Plants, Regulatory Guide 1.76, U.S. Atomic Energy Commission (1974).
2. Standard Review Plan: Missiles Generated by Natural Phenomenon, Section 3.5.1.4 (Rev. 1), U.S. Nuclear Regulatory Commission, Office of Nuclear Reactor Regulation (1976).
3. A. Stephenson, Full-Scale Tornado-Missile Impact Tests, EPRI NP-440, Sandia Laboratories, Tonopah, Nev. (1977).
4. F. A. Vassallo, Missile Impact Testing of Reinforced Concrete Panel, Calspan Corporation, Buffalo, N.Y. (1975).
5. A. Stephenson, Tornado Vulnerability Nuclear Production Facilities, Sandia Laboratories, Albuquerque, N.M. (1975).
6. A. Stephenson, Full Scale Tornado Missile Impact Tests, EPRI NP-14B, Sandia Laboratories, Tonopah, Nev. (1976).
7. A. Stephenson, Full Scale Tornado Missile Impact Tests, EPRI RP-399, Sandia Laboratories, Tonopah, Nev. (1976).
8. D. K. Tu and R. C. Murray, Numerical Simulations of Tornado-Borne Missile Impact, UCRL-52223, Lawrence Livermore Laboratory, Livermore, Calif. (1977).
9. Y. M. Gupta and L. Seaman, Development of Dynamic Constitutive Relation for Reinforced Concrete, Stanford Research Institute, Menlo Park, Calif. (1975).
10. Dynamics of a Blunt Projectile Impacting Concrete at 1400 Feet Per Second, Physics International Co., San Leandro, Calif. (1975).
11. J. O. Hallquist, *DYNA2D--An Explicit Finite Element and Finite Difference* Code for Axisymmetric and Plane Strain Calculators (User's Guide), UCRL-52429, Lawrence Livermore Laboratory, Livermore, Calif. (1978).
12. Y. M. Gupta and L. Seaman, "Local Response of Reinforced Concrete to Missile Impacts," 4th International Conference on Structural Mechanics in Reactor Technology, Vol.J(b), International Association for Structural Mechanics in Reactor Technology and Commission of European Communities, Brussels, Belgium (1977).

13. S. W. Key, HONDO--A Finite Element Computer for Large Deformation Dynamic Response of Axisymmetric Solids, Sandia Laboratories, Albuquerque, N.M. (n.d.).
14. Y. M. Gupta and L. Seaman, A Generalized Plasticity Model for Predicting Failure of Concrete, SRI International, Menlo Park, Calif. (1976).
15. K. D. Birkimer and R. A. Lindeman, "Dynamic Tensile Strength of Concrete Materials," American Concrete Institute Journal, 68, 1 (1971).

REFERENCES

A Generalized Cap Model for Geological Materials, DNA 3443T, Weidlinger Associates, New York, N.Y. (1974).

M. Alderson et al., "Reinforced Concrete Behavior Due to Missile Impact," 4th International Conference on Structural Mechanics in Reactor Technology, Vol. J(b), International Association for Structural Mechanics in Reactor Technology and Commission of European Communities, Brussels, Belgium (1977).

I. Attalla and B. Nowothy, "Missile Impact on Reinforced Concrete Structure," Nuclear Engineering and Design, 37, 3 (1976).

J. Dubois, J. Chedmail, and J. Bianchini, "Numerical Analysis of Impact-Penetration Problems for Nuclear Reactor Safety," 4th International Conference on Structural Mechanics in Reactor Technology, Vol. J(b), International Association for Structural Mechanics in Reactor Technology and Commission of European Communities, Brussels, Belgium (1977).

C. Kot, "Spalling of Concrete Walls Under Blast Loads," 4th International Conference on Structural Mechanics in Reactor Technology, Vol. J(b), International Association for Structural Mechanics in Reactor Technology and Commission of European Communities, Brussels, Belgium (1977).

P. McHahon, B. Meyers, and K. Buchert, "The Behavior of Reinforced Concrete Barriers Subjected to the Impact of Tornado Generated Deformable Missiles," 4th International Conference on Structural Mechanics in Reactor Technology, Vol. J(b), International Association for Structural Mechanics in Reactor Technology and Commission of European Communities, Brussels, Belgium (1977).

SFS/ej